Interfacial Fracture Toughness Measurement of New Composite Material SnSb11Cu6/ 20Steel

Yuepeng Gao, Jianmei Wang, Yuyang Liu

Engineering Research Center of Heavy Machinery Ministry of Education, Taiyuan University of Science and Technology, Taiyuan, 030024, China

Abstract: The interface fracture toughness test of SnSb11Cu6/20steel is realized by three-point bending experimental technique, interfacial cracks are introduced through the overall bending of the composite panel, and the critical energy release rate of 12.07×10^3 J/m^2 is obtained by calculating the energy released per unit area at the fracture interface. To characterize the stress state of the crack tip, the stress phase angle of the crack tip is calculated using finite element analysis(FEA). At the same time, five sets of FEA experiments are specifically set up to determine the magnitude of the effect of changes in the interface fracture critical load values on the critical energy release rate. The results show that the change in the critical load value affects the critical energy release rate by only 0.08%. And the characterization of the crack tip stress state reveals that the relative strength of the shear stress that drives the interfacial cracking is weaker than that of the positive stress after the crack propagates to a certain length under bending conditions, which also implies that the positive stress is the main reason that drives the interfacial crack to continue propagating when the composite layer is completely fractured.

Keywords: Three-point bending; Interfacial fracture toughness; Fracture mechanics; Critical loading; Energy release rate; Cohesion models

---

*Corresponding author. School of Mechanical Engineering, Taiyuan University of Science and Technology, No 66, Waliu Road, Wanbailin District, Taiyuan City,Shanxi Province, Taiyuan, 030024, China. E-mail addresses: wjmhdb@163.com (Janmei Wang), YuepengGao@163.com (Yuepeng Gao).

1 Introduction

Oil-film bearing is widely used in the key equipment of iron and steel, mine, metallurgy, electric power, and so on, because of its advantages of low friction coefficient, low loss and high-rigidity [1]. Oil-film bearing is the core load-carrying component of many kinds of key equipment, the interface bonding performance of its Babbitt layer and steel body is vital to the stable operation of devices [2]. Due to the difference in the mechanical properties of the metals on both sides of the bonding interface, under uneven temperature and unstable external loads, a strong residual stress field is likely to be generated at the bearing bonding interface end, which will adversely

affect the bonding performance of the interface[3]. As the core component of the oil film bearing, the structure and the force during operation play a vital role in the final performance of bearing. Therefore, it has very important guiding significance for enterprise production and engineering applications to study the interface fracture toughness of bearing bushing and babbitt alloy and improve their bonding strength.

Parameters such as G ("fracture energy" or "strain energy release rate") and K ("stress intensity factor") are often determined and presented in connection to fracture mechanics studies [4]. Griffith [5] assumed that fracture occurs when sufficient mechanical energy is released from a stress field, energy that is used to form new fracture surfaces when a crack propagates. The released energy comes from stored elastic or potential energy of the loading system and can, in principle, be calculated for any type of test piece. Such a determination results in a measure of the energy required for extending a crack over a unit area and that value is termed the toughness or critical strain energy release rate (denoted G_c, unit J/m^2) [6].

M.E.M Zebar et al.[7] used the four-point bending method to study the interface fracture toughness of aluminum alloy/PMMA polymer and aluminum alloy/stainless steel in the steady state and transient state, and explored the crack delamination under the condition of exceeding the internal load point and extended the measurement of the interface fracture toughness, and tried to reveal the reason why the interface fracture toughness has a strong dependence on the phase angle. Panayiotis Tsokanas et al.[8] used the double cantilever beam (DCB) and notched end bending test method to conduct an experimental study on the interface fracture toughness of the new titanium-carbon fiber reinforced plastic bonded joint, considering the effect of bending-extension coupling and the residual thermal stress caused by manufacturing on the fracture toughness of joints, and the load-displacement response, fracture behavior and fracture toughness of the materials in the test under four manufacturing schemes were compared. Harpreet S. Bedi et al. [9] used carbon nanotubes to design the interphase microstructure of carbon fiber/epoxy composites, and tested the fracture toughness of the interface. The experimental results showed that the relative improvement of the

interphase fracture toughness depends on the microstructure of the interphase, and concluded that the use of carbon nanotubes for interphase structure design was an excellent tool to accurately adjust the average interface characteristics of composite materials.

Evelise M.Souza et al.[10] used four-point bending and micro-tensile tests to study the interfacial fracture toughness and micro-tensile strength of composite cements bonded to dentin, and proposed the etch-and-rinse and 'universal' self-etch composite cements per-formed best. The micro-tensile bond strength and interfacial fracture toughness tests did not correlate well. Pulin Nie et al. [11] used the elastoplastic theory and **FEA** method to study the effect of residual stress on the energy release rate that characterized the adhesion strength of coatings to substrates. The results showed that the residual stresses can influence considerably both the energy release rate and the phase angle, The features of variation of the energy release rate with respect to the residual stresses were influenced by the critical buckling stress, and the geometry of the cracked system that includes the sizes of the crack and the central deflection. Shaobin Wang et al.[12] studied the interfacial fracture toughness of sintered hybrid silver nanoparticles(AgNPs) on both Au and Cu substrates as a function of sintering temperature, and both porosity and pore sizes of the sintered silver interconnects were analyzed across the micro- and macro-length scales and related to the interfacial fracture toughness, which permits to predict the fracture toughness of the sintered silver interconnects. However, up to now, there is less literature on the fracture toughness of Babbitt alloy and steel body of oil-film bearing bushing at home and abroad. Therefore, it is necessary to conduct an in-depth analysis of the fracture toughness of Babbitt and steel body.

Fracture toughness tests have been widely used to investigate ceramics, composites, glass-ionomers, as well as enamel and dentin–composite adhesive interfaces [13]. In this study, with Sn-based Babbitt alloy SnSb11Cu6 and 20steel bimetallic composite plate as the research object, the simulation analysis, with or without crack propagation of interface , was done using **3PB** test method. By comparing the results of finite

element simulation with and without crack propagation (load vs deflection curve) at the interface inorder to obtain the critical load value for interface fracture. At the same time, combined with the virtual crack propagation theory and the established fracture mechanics model, the critical energy release rate for interface crack initiation was calculated. The finite element simulation results were basically consistent with the experimental results. Therefore, the experimental methods and theoretical models used in the assessment of the fracture toughness of the Babbitt alloy/steel body interface are reliable.

2 Experimental process

The **3PB** experiment is performed to deduce the crack formation process of at the SnSb11Cu6/20steel bonding interface, and to study the fracture toughness of the bonding interface, so as to evaluate the bonding performance of Babbitt alloy SnSb11Cu6 /20steel. Based on the above research content, this paper proposed a controllable crack formation method, and used an appropriate mechanical model to calculate the energy release rate of the interface crack and the stress phase angle at the crack tip [14].

2.1 Material preparation and experimental technology

The experimental materials were Babbitt alloy and 20steel, which were the oil film bearing bushing materials. Babbitt alloy layer forming differs from the conventional casting process. but using a new welding process to weld the material layer by layer to the steel plate. With this technology, the bond strength of the interface is greatly improved, thus increasing the life of the bushing and reducing production costs. the babbitt alloy material composition is shown in Table 1. In the **3PB** experimental method employed, the SnSb11Cu6 layer is the stretched layer, i.e., the composite layer, and the 20 steel is the compressed layer, i.e., the matrix layer.The sample size is: SnSb11Cu6 layer: 192mm×25mm×5mm; steel20: 192mm×25mm×10mm. The sample size is shown in Figure 1 (a), a total of 4 samples were prepared, and the model of 3PB tests is shown in Figure 1(b).

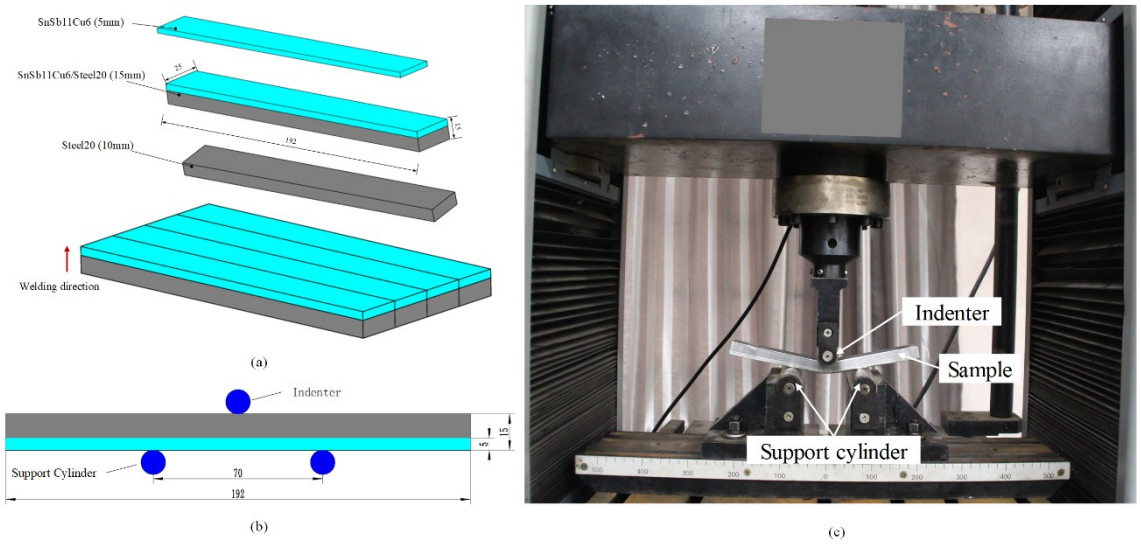

Figure 1 (a) Dimensions of tensile specimen , (b)Schematic diagram of **3PB**, and (c) Electronic universal testing machine

Table 1 Babbitt alloy material composition

SnSb11Cu6	**Chemical composition (%)**									
	Sn	Pb	Sb	Cu	Fe	As	Bi	Zn	Al	Cd
	balance	0.35	10.0~12.0	5.5~6.5	0.08	0.05	0.05	0.005	0.005	0.05

The **3PB** test was completed on the microcomputer-controlled electronic universal testing machine WDW-E100D. Among them, the radius of the indenter applying the load was 12mm, which was located in the middle above the steel plate. The two supporting cylinders were located under the SnSb11Cu6 layer with a distance of 70mm (as shown in Figure 1(c)). The indenter applied a load to the 20 steel layers at a speed of 1mm/min. During the bending process of the composite board, a high-definition camera was used to continuously photograph the fracture process of the bonding interface and the SnSb11Cu6 layer. When the specimen was bent to the maximum deflection, the crack stopped expanding, and then the specimen was removed. the length of the fractured interface was measured with a VHX-2000C metallurgical microscope, as shown in Figure 2.

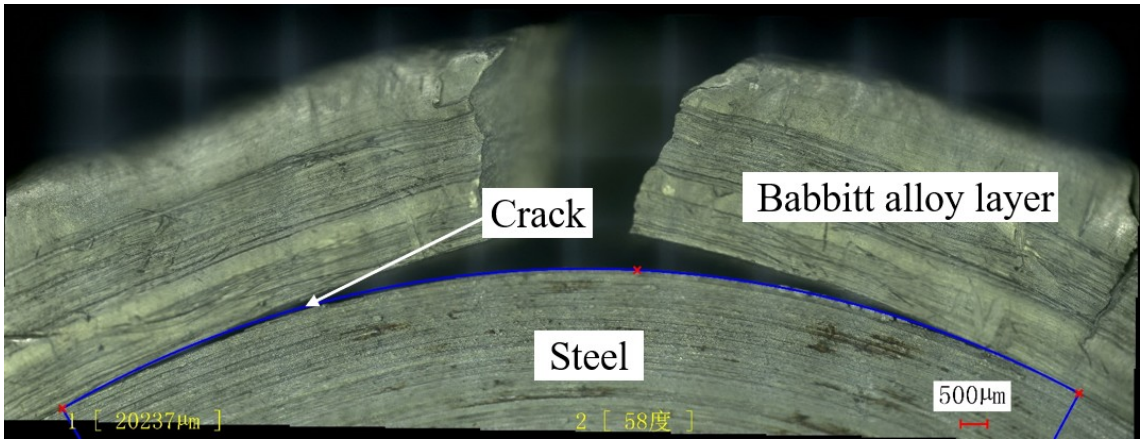

Figure 2 Measuring the length of the fracture interface

2.2 Fracture mechanism

During the bending process of the specimen, the steel matrix layer transferred the load applied by the indenter to the babbitt alloy layer through the bonding interface. The babbitt alloy layer would generate larger tensile stress, and at the same time, the bonding interface would generate shear stress. Under the continuous action of external load, the specimen would undergo elastoplastic deformation. Therefore, the system would continuously accumulate the strain energy generated by deformation. When the strain energy accumulated to the limit that the system can withstand, it would find the weakest part of the system to release energy. Since the weakest part of the SnSb11Cu6/20 steel system was at the bonding interface, the strain energy was released at the bonding interface. The crack nucleation place was naturally the junction interface.

However, there were two paths for the crack to continue to expand. The first was to expand to the base layer; the second was to expand along the bonding interface. Since the energy consumed by the expansion along the interface was less than that along the base layer, cracks tend to expand along the path that consumes less energy, that is, the bonding interface. As the bending process continued, the energy of the system continued to rise. At this time, the relatively weak composite layer also began to crack initiation and expanded along the direction perpendicular to the interface, and finally merged with the interface crack to form a main crack. The crack initiation process is shown in the figure 3.

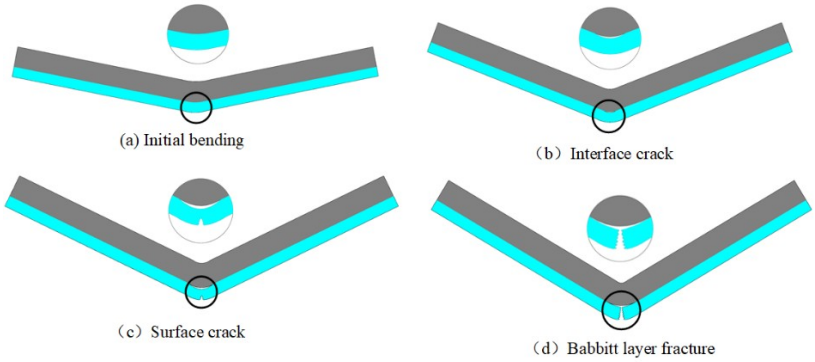

Figure 3 Interface crack initiation process

2.3 Fracture mechanics model

The energy release rate (G_{ci}) is the rate at which the strain energy released during crack propagation changes relative to the crack area expansion. Therefore, it can be used to determine the interface binding energy of Babbitt alloy/steel matrix. Calculate the energy required for the crack propagation unit surface area, the expression is as follows [15]:

$$G_{ci} = -\frac{\Delta \Pi}{\Delta A}, \qquad (1)$$

where ΔA is the surface area of the crack propagation, $\Delta \Pi$ is the potential energy released by the system when the crack propagates. The potential energy includes the energy ,U ,consumed by the deformation of the SnSb11Cu6/20 steel system and the work done by the external force F. The expression is as follows:

$$\Pi = U - F \qquad (2)$$

Since the indenter applies a constant displacement load, there is no extra work on the crack propagation from the outside, so F=0, Then, $\Pi = U$ .Therefore, (1) formula can be expressed as:

$$G_{ci} = -\frac{\Delta U}{\Delta A} \qquad (3)$$

From the perspective of actual bonding, the energy consumption , U, used to separate the interface in an elastoplastic system consists of the elastic energy ,Ue ,and the energy dissipated by plastic deformation, Up ,[16]. therefore,

$$G_{ci} = -\frac{\Delta U_e + \Delta U_p}{\Delta A} \quad (4)$$

The phase angle represents the relative strength of the normal stress and the shear stress at the crack tip, and is a supplementary parameter that characterizes the bonding strength. In general, Gci changes with the phase angle. In the two-dimensional plane problem, the phase angle is expressed as [17]:

$$\psi = \arctan\left(\frac{\sigma_{12}}{\sigma_{22}}\right) \quad (5)$$

3 Experimental results and discussion

During the 3PB test, the electronic universal testing machine recorded the change in the indenter load and the deflection of the sample center over time, and plotted the load-deflection curve. The curve depicts the four stages from instability to failure of the SnSb11Cu6/20 steel system. The cracks mainly initiate and propagate in the latter two stages, which are the initial elastic deformation stage (Figure 3(a)), plastic deformation stage (interface crack initiation) (Figure 3(b)), crack initiation and propagation stage of the composite layer (Figure 3(c)), the final stage of the fusion of composite layer cracks and interface cracks (Figure 3(d)).

This process is shown by the load-deflection curve, As shown in Figure 4. The deflection curve is a linear region with a small distance before point A. However, plastic deformation occurs between point A and point B, where point A is the yield point of the system. In addition, since the strength of the bonding interface of the SnSb11Cu6/20 steel system is far less than that of Babbitt alloy, the initiation of interface cracks occurs before the fracture of the Babbitt alloy, i.e., in the AB section of the curve. Between point B and point C is the comprehensive stage of plastic deformation of the system and

crack propagation at the bond interface. After observation, point B is the initiation time of the surface crack of the babbitt alloy. Point C is the moment when the babbitt alloy layer crack and the interface crack merge to form the main crack. The picture inserted in Figure4 corresponds to the interface crack state at the point of maximum load. After point C is the large deformation failure stage of the steel matrix, which will not be repeated here.

In the process of specimen bending, although there is a fracture phenomenon of the bonding interface, the occurrence of this phenomenon will lead to a sudden increase in the deflection of the specimen and a sudden decrease in the load. As a matter of common sense, this phenomenon is directly reflected drop phenomenon on the curve[18]. However, due to the sensitivity limitation of the experimental machine, the moment when the interface crack occurs is not directly reflected on the load-deflection curve. In the AB section of the curve, it can be seen that as the deflection of the center of the curve increases, the load slowly rises. Therefore, it is difficult to determine the critical load of interface crack initiation directly on the curve. In order to determine the critical load value of crack initiation at the bonding interface of SnSb11Cu6/20 steel during specimen bending, in the following research work, the experimental results and FEA will be combined to finally determine the critical load value.

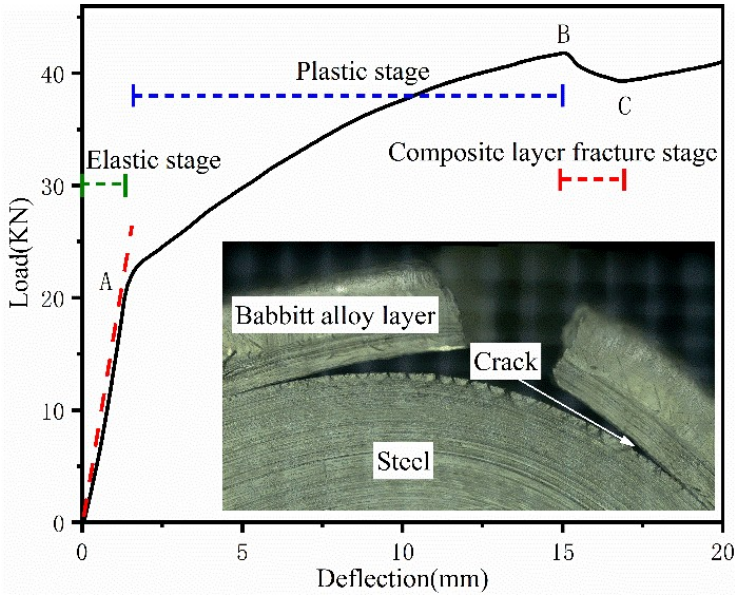

Figure 4 The load vs deflection curve of the 3PB test (NO.1 sample). the illustration shows the fracture interface corresponding to the maximum deflection of the specimen

3.1 Calculation of fracture toughness of bonding interface

Because of the particularity of the research object, it is difficult to precisely control the required length of interfacial crack propagation. so, the critical energy release rate and the phase Angle of the crack tip is calculated by using the elastic mechanics method is more difficult under the elastic-plastic condition. Therefore, the FEA method is used to calculate the fracture mechanics model of this study[15]. The load-deflection curve in Figure 4 shows the nonlinear characteristics of the AB section, which is mainly caused by the combined effect of the plastic behavior of the SnSb11Cu6/20 steel matrix material and the interface cracks. This paper uses FEA to analyze the elastoplastic behavior of SnSb11Cu6/20steel system and calculates the fracture toughness of the interface.

The FEA software used in this paper is ABAQUS, and it has successfully calculated the energy release rate of the crack at the bonding interface by using its strong nonlinear analysis and calculation capability[20]. The element type of the finite element model is hexahedral C3D8R, the middle bonding layer of SnSb11Cu6/20 steel is cohesive elements, and the element type is COH3D8. Among them, the indenter that applies the load and the two supporting cylinders are defined as analytical steel bodies, as shown in Figure 5(a). In order to improve the accuracy of calculations, the composite plate adopts a progressive meshing method, Partial subdivision of cohesive cells with a grid size of 0.5mm. and the rest are symmetrically distributed, the unit size is 1mm and 2mm respectively (Figure5(b)). According to the length of the crack, a cohesive layer is only established in the finite-length bonding surface of the model (Figure5(c)). The red marking line in Figure 5(a) is the position where the cohesive unit is embedded.

Firstly, under the condition of interfacial crack propagation, the elastoplastic state of SnSb11Cu6/20 steel system with crack propagation in the bending process was

studied by using finite element method to simulate the bending process of the sample. The input parameters of the model include the mechanical properties of the composite layer, the matrix layer and the bonding interface. The elastoplastic mechanical properties of two different materials need to be obtained by standard tensile experiments. As for the cohesive unit properties of the bonding layer, such as shear strength and fracture strength, both are obtained through related experiments. Finally, the load-deflection curve of the model can be output in the simulation results. The load-deflection curve shown in Figure 6 is the simulation result of one of the four specimens.

Due to the microscopic defects of the material itself and the real error between the experimental conditions and the simulated environment, there is a slight deviation in the agreement between the two curves at key points. However, the two curves remain consistent in the overall development trend. In the initial stage of the curve (before the deflection reaches 1.8mm), the SnSb11Cu6/20 steel sample is in the elastic stage as a whole. When the deflection reaches 1.8mm, the specimen enters the plastic yield stage. Next, finite element simulation will be carried out on the assumption that the interface is crack-free to determine the separation point of the two curves, namely, to determine the load value of interface crack initiation.

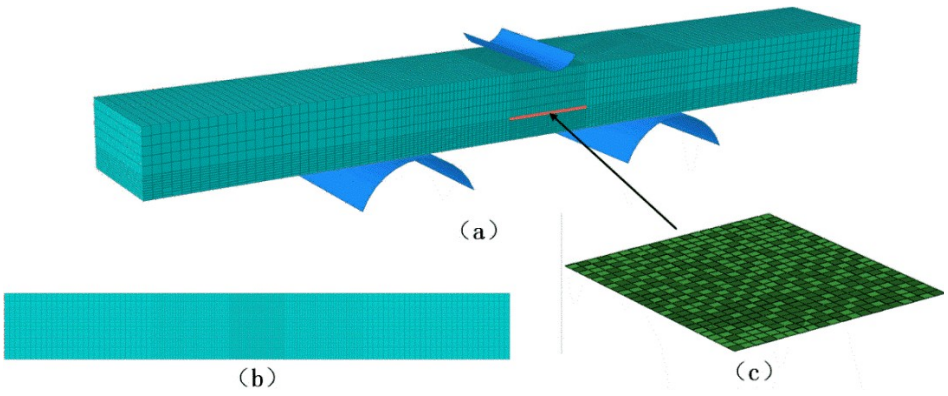

Figure 5 (a) **FEA** model, (b) Progressive mesh refinement , and (c) Cohesion grid cells

By simulating the elastoplastic behavior of the system under the condition that there is no crack propagation at the interface, the load-deflection curve of the system is obtained, as shown in Figure7. Due to the formation of cracks, the stiffness of the

SnSb11Cu6/20 steel system is weakened. Then, during the bending of the specimen, the load acting on the specimen without interfacial crack formation is greater than the specimen with interfacial crack initiation. Therefore, the load corresponding to the separation point of the two curves at the initial stage should be the critical load for the initiation of interface cracks. However, due to the interference of objective factors such as experimental error and the simplification of the analysis model, it is difficult to directly determine the precise separation point of the two curves and the corresponding critical load value. Therefore, only an approximate critical load value can be determined by this method, for example, the separation point marked in the inset of Figure 7 is 1.8mm and the load is 25.5KN. Although the critical load value is approximate, it does not affect the calculation of the energy release rate of the system interface crack. The specific reasons will be detailed in the discussion section.

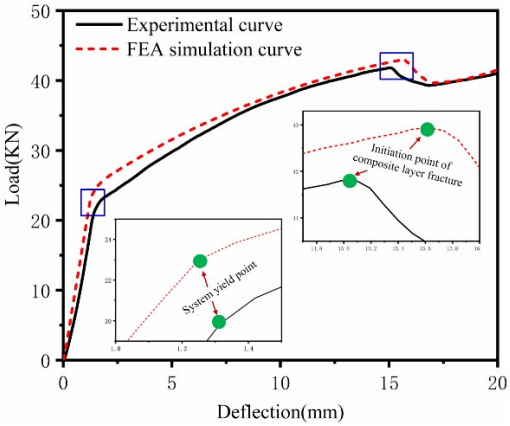

Figure 6 Comparison of the load vs central deflection curves derived from FEA simulation (with interfacial crack propagation) and experimental results (NO. 1

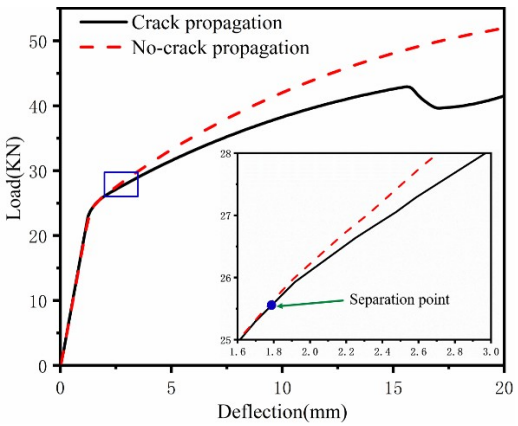

Figure7 Comparison of the load vs central deflection curves derived from FEA simulation with and without interfacial crack propagation (NO.1 sample)

After the critical load of interface cracking is determined, the debonding process of specified cracks at the interface is simulated to further study the crack initiation and propagation process during the bending process of the system. Until the applied load value reaches the critical load value of the interface fracture, the composite layer and the matrix layer is always bonded together by the cohesive layer. When the load reaches the fracture value of the interface, the crack propagation ability of the cohesive layer is activated. As the sample continues to bend to the specified deflection, the interface

crack will also expand to the corresponding length. Then, the load-deflection curve and the energy consumed in the bending process are calculated simultaneously. The equivalent stress cloud diagram of the FEA and calculation results is shown in Figure 8. Because it is a nonlinear simulation, the crack initiation site is uncontrollable, so, interfacial cracking does not occur at the maximum flexural part of the joint interface and exhibits left-right symmetry. However, the destruction process of the system is consistent with the experimental results.

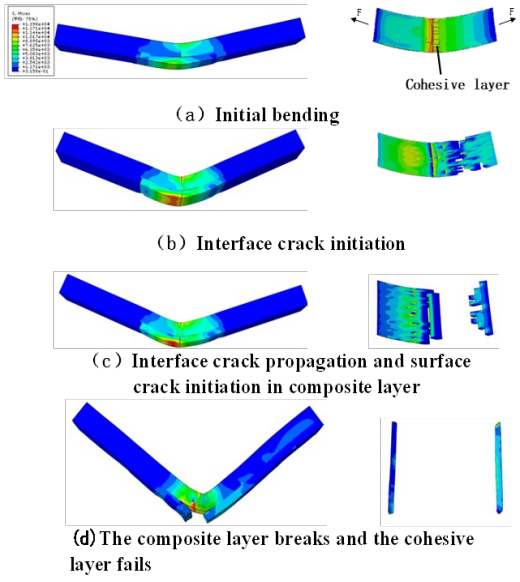

Figure 8 Stress cloud diagram from **FEA** results(NO.1 sample)

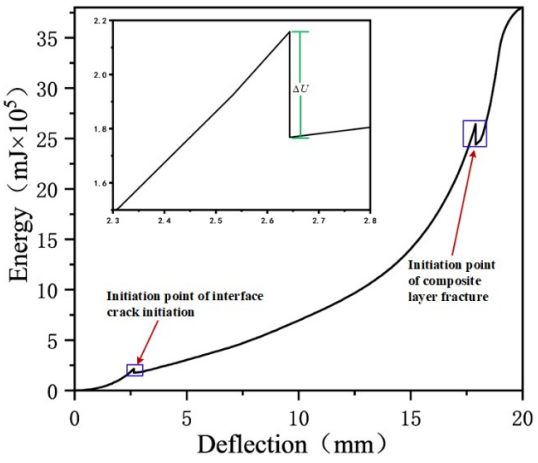

Figure 9 Energy vs deflection curve from **FEA** (NO.1 sample). the illustration shows the energy consumed during spontaneous expansion of interface cracks.

During the bending of the specimen, the energy value of the system will continue to rise with the continuous increase of the external load. When the deflection of the system reaches the maximum value, the energy value also reaches the maximum, as shown in Figure 9. In order to assist in calculating the energy release rate of the interface crack, the interfacial crack was forced to spontaneously extend over a small length (0.85 mm) after the completion of the loading [15,16]. In this spontaneous stage, the released energy is used to generate a new crack surface. This sudden decrease in energy value can be reflected in the sudden drop of the curve, as shown in the illustration in Figure 9. Since the interface crack initiation is near the yield critical point

of the system, the point at which the energy value of the system suddenly drops is set at the interface crack initiation point. When the curve deflection reaches about 16mm, the babbitt alloy layer is completely broken. Similarly, the energy value of the system also decreases sharply (this phenomenon can be directly detected by the experimental instrument.

According to the energy released by the system and the change of the crack area, the energy release rate of the interface can be calculated by formula (3). In most cases, the resistance to interface crack growth of SnSb11Cu6/20steel system will change with the state change of crack tip stress [12]. Therefore, it is also necessary to measure the stress state of the crack tip corresponding to the critical energy release rate. According to the stress component of the crack tip, the stress phase Angle of the crack tip is calculated by using formula (5), and then the stress state of the crack tip is described. Table 2 shows the specific data obtained during the bending experiment of the 4 samples. The calculated average energy release rate is 12.07×103 J/m2 and the stress phase angle is 29.77°.

Table 2 Mechanical property estimations of SnSb11Cu6/20 steel substrate system from 3PB tests

NO.	*dP/dw* (10^3N/mm)	D_0 (mm)	D (mm)	L (mm)	G_{ci} (10^3J/m^2)	ψ (°)
1	12.21	1.86	20.10	20.7	12.06	29.66
2	12.84	1.84	19.96	19.8	12.09	29.77
3	12.52	2.85	20.03	20.2	12.02	29.86
4	12.86	1.84	19.98	19.9	12.09	29.77
Average	12.61	1.85	20.02	20.15	12.07	29.77

In Table 2, *dP/dw* is the slope of the load vs displacement curve at the initial elastic stage of the sample, D_0 is the critical deflection value corresponding to the crack initiation at the sample interface, D is the maximum deflection value during the bending process of the specimen. L is the length of the entire crack at the sample interface. G_{ci} is the critical energy release rate, ψ is the stress phase angle at the crack tip.

The slopes of the curves of the 4 specimens at the initial stage of the bending process are calculated, as shown in Table 2. Among them, D0 is the data obtained by comparing the curve under the condition of FEA with or without crack growth. Gci and

ψ are obtained with the help of finite element calculation results and combining formulas (3) and (5).

3.2 Discussion

The mechanical analysis of the SnSb11Cu6/20steel model requires the length of crack propagation, the load corresponding to the maximum deflection of the sample, the critical load corresponding to the initiation of interface cracks, and the mechanical properties of the composite layer and the matrix layer. Whether the above parameters can be accurately measured will affect the calculation of interface fracture toughness. Therefore, it may be more difficult to determine the precise critical load. However, whether the error of this parameter will have a great influence on the calculation result, it will be discussed next.

In this paper, by comparing the load-deflection curves obtained by finite element simulations assuming no interface crack growth and that with interface crack growth under the same conditions, the approximate critical load for interface crack initiation is determined. According to fracture mechanics [15], when the driving force of crack propagation is equal to the resistance of the crack, the critical energy release rate is determined by the transition of the crack from a steady state to an unstable state, and has nothing to do with the fracture process [21,22]. Taking the first sample in Table 2 as an example, the critical load varies from 0 to 10 mm (45% of the maximum deflection of 20 mm), its impact on energy release rate is only 0.08%, as shown in Table 3. Since the precise critical load has little effect on the energy release rate, the effect of errors related to the precise critical load can be ignored.

In the FEA, characterized by the maximum crack length and central deflection, the change of the critical load has a small effect on the energy release rate of the crack in a fixed transition state. In fact, many analytical problems about the energy release rate during interface cracking have been studied through approximate models, for example,

the well-known bubble test method [17,23], which simplifies the cracking process of a flat plate with a fixed length during bending. Therefore, for convenience, it can be assumed that in the 3PB experiment, the beginning of crack initiation is the beginning of bending without losing the accuracy of the energy release rate. In addition, because the crack growth will be unstable under high external load rates, high-speed loading should be avoided during the loading process [19].

Table 3 Energy release rates with respect to different critical central deflections

D_0(mm)	1	3	5	7	9
G_{ci}($J\times10^3/m^2$)	12.05	12.08	12.07	12.06	12.08

The fracture toughness analysis of the interface requires a controllable interface cracking mode. In the 3PB test of this paper, the fracture toughness of the interface is far less than that of the composite layer babbitt alloy, so the crack initiation is the first at the interface. And due to the difference in the mechanical properties of the materials on both sides of the interface, the bonding interface is subject to great shear stress. Under the continuous load of the indenter, the interface cracks continue to expand until the external load stops acting. Similar cracking phenomenon was also observed in other bending tests. However, the cracking configuration may not always be the case.

According to the crack propagation mechanism, the crack is more likely to grow along the path that consumes less energy, and the mechanical properties of SnSb11Cu6/20steel system can affect the interface cracking mode. The cracks in the composite layer will propagate in the direction perpendicular to the interface until it blends with the interface cracks. At this time, the interface constraints are completely dissipated. Therefore, the composite layer with higher fracture toughness and the path with lower resistance are more conducive to the continuous crack propagation along the interface. In addition, the stress state at the crack tip will change with the crack propagation, which will also affect the crack path. Although the propagation path of the crack is uncertain, this property limits its application in many experiments. However, the 3PB experiment method used in this research has the advantages of simple operation, short test time, and a reliable fracture model.

4. Conclusion

(1) Based on the 3PB test, the fracture toughness of the bonding interface of oil film bearing bushing material SnSb11Cu6/20 steel system (made by welding technology) has been measured successfully. By comparing the load-deflection curve of finite element simulation with and without interface crack propagation, the approximate deflection value and load value of interface crack initiation are determined, which are 1.85mm and load 25.5KN respectively.

(2) In order to determine the influence of the accuracy of critical load on the energy release rate of interface crack, five groups of critical deflection values (within 48% of the maximum deflection value) are set. It is calculated that the impact of the critical load value on the energy release rate is only 0.08%, Therefore, the accuracy of the critical load value has a negligible effect on the energy release rate of the crack.

(3) This paper also characterizes the stress state of the interface crack tip by calculating the stress phase angle. The calculated average stress phase angle is 29.77°, indicating that when the crack expands to a certain length under bending conditions, the relative strength of the shear stress that promotes the interface cracking is weaker than Normal stress, which also implies that when the composite layer is completely fractured, positive stress is the main reason that drives the continued propagation of interfacial cracks.

Acknowledgements

The financial support by the National Natural Science Foundation of China is gratefully acknowledged (Grant No. 51875382 and 52035006); We also thank the financial support provided by The Shanxi Province Sixth Batch Emerging Industry Leading Talents (Innovative) Funding Project (Grant No. 202006).

References

[1] Xia Quanzhi, Wang Jianmei, Yao Kun, Hou Dingbang, Li Zhixiong. Interface bonding properties of multi-layered metal composites using material composition method. Tribol Int 2019; 13:251-257.

[2] Jianmei Wang , Fanning Meng, Xiaotian Zhang, Yinan Liang, Zhixiong Li. Mathematical model and algorithm of interface singular stress field of oil-film bearing. Tribol Int 2017; 116:351-361.

[3] W.O.SOBOYEJO, G.-Y.LU, S.CHENGALVA, J.ZHANG, V.KENNER . A modified mixed-mode bending specimen for the interfacial fracture testing of dissimilar materials. FFEMS 1999; 22: 799–810.

[4] Karl-Johan Soderholm. Review of the fracture toughness approach. Dental Materials 2010; 26: e63-e77.

[5] A. A. Griffith. The phenomena of rupture and flow in solids.Phil Trans R Soc Lond Ser A 1921;221:168–98.

[6] H.V.TIPPUR, L.Xu. INTERFACIAL CRACK INITIATION UNDER QUASI-STATIC AND DYNAMIC LOADING CONDITIONS: AN EXPERIMENTAL STUDY. FFEMS 1997; 20: 49-60.

[7] M. E. M. Zebar, M. L. Hattali, N. Mesrati. Interfacial fracture toughness measurement in both steady state and transient regimes using four-point bending test. International Journal of Fracture 2020; 221:168–98.

[8] Panayiotis Tsokanas, Theodoros Loutas1, Peter Nijhuis. Interfacial Fracture Toughness Assessment of a New Titanium–CFRP Adhesive Joint: An Experimental Comparative Study. Metals 2020;10(5),699.

[9] Harpreet S. Bedi, Beant K. Billing, Prabhat K. Agnihotri. Interphase engineering in carbon fiber/epoxy composites: Rate sensitivity of interfacial shear strength and interfacial fracture toughness. Polymer Composites 2020; 41:2803-2815.

[10] Evelise M, Souzaa, Jan De Muncka, Pong Pongprueksa, Annelies Van Ende, Bart Van Meerbeek. Correlative analysis of cement–dentin interfaces using an interfacial fracture toughness and micro-tensile bond strength approach. Dental Materials 2016; 32:1575-1585.

[11] Pulin Nie, Yao Shen, QiuLong Chen, Xun Cai. Effects of residual stresses on interfacial adhesion measurement. Mechanics of Materials 2009; 41:545-552.

[12] Shaobin Wang, Christoph Kirchlechner, Leon Keer, eat al. Interfacial fracture

toughness of sintered hybrid silver interconnects. Electronic materials 2019; 55:2891-2904.

[13] Evelise M. Souza, Jan De Munck, Pong Pongprueksa, eat al. Correlative analysis of cement–dentin interfacesusing an interfacial fracture toughness andmicro-tensile bond strength approach. Dental Materials 2016; 32:1575-1585.

[14] C.P.S.Porto, M.P.L.Parente, R.M.N.Jorge, L.C.Pereira, S.Griza. Fracture toughness of the interface between Ni-Cr/ceramic, alumina/ceramic and zirconia/ceramic systems. FFEMS 2016; 39: 817-829.

[15] Anderson, TL, Fracture Mechanics: Fundamentals and Applications. CRC Press, Boca Raton 1995.

[16] Hutchinson, JW, Suo, Z, ‘‘Mixed Model Cracking in Layered Materials.’’ Adv. Appl. Mech 1992; 29:63–91.

[17] Elizald, MR, Sa´nchez, JM, Martı´nez-Esnaola, J, et al.Interfacial Fracture Induced by Cross-sectional Nanoindentation in Metal-Ceramic Thin Film Structures. Acta Mater 2003; 51:4295–4305.

[18] Hutchinson, JW, Suo, Z. Mixed Model Cracking in Layered Materials. Adv. Appl. Mech 1992. 29: 63–91.

[19] Shaviv, R, Roham, S, Woytowitz, P. Optimizing the Precision of the Four-point Bend Test for the Measurement of Thin Film Adhesion. Microelectro. Eng. 2005; 82: 99–120.

[20] ABAQUS, Reference Manuals, Version 6.5. Hibbit, Karlsson and Sorensen, Providence, RI 2004.

[21] Parks, DM. The Virtual Crack Extension Method for Nonlinear
Material Behavior. Comp. Meth. Appl. Mech. Eng 1997; 12:353–364.

[22] Hellen, TK. On the Method of Virtual Crack Extensions. Int. J. Num. Meth. Eng 1975; 9: 187–207.

[23] Jensen, HM. The Blister Test for Interface Toughness Measurement. Eng. Fract. Mech 1991. 40: 475–486.